HHS Public Access

Author manuscript

Nano Lett. Author manuscript; available in PMC 2024 September 13.

Published in final edited form as:

Nano Lett. 2023 September 13; 23(17): 7941–7949. doi:10.1021/acs.nanolett.3c01775.

Cancer Cell Membrane Nanodiscs for Antitumor Vaccination

Zhongyuan Guo[†],

Ilkoo Noh[†,#],

Audrey T. Zhu,

Yiyan Yu,

Weiwei Gao,

Ronnie H. Fang[*], **Liangfang Zhang**[*]

Department of NanoEngineering, Chemical Engineering Program, and Moores Cancer Center, University of California San Diego, La Jolla, CA 92093, USA

Abstract

Cell membrane-based nanovaccines have demonstrated attractive features due to their inherently multiantigenic nature and ability to be formulated with adjuvants. Here, we report on cellular nanodiscs fabricated from cancer cell membrane and incorporated with a lipid-based adjuvant for antitumor vaccination. The cellular nanodiscs, with their small size and discoidal shape, are readily taken up by antigen-presenting cells and drain efficiently to the lymph nodes. Due to its highly immunostimulatory properties, the nanodisc vaccine effectively stimulates the immune system and promotes tumor-specific immunity. Using a murine colorectal cancer model, strong control of tumor growth is achieved in both prophylactic and therapeutic settings, particularly in combination with checkpoint blockades. Considerable therapeutic efficacy is also observed when treating a weakly immunogenic metastatic melanoma model. This work presents a new paradigm for the design of multiantigenic nanovaccines that can effectively activate antitumor immune responses and may be applicable to a wide range of cancers.

Graphical Abstract

[*]Corresponding authors: rhfang@ucsd.edu or zhang@ucsd.edu.
[†]These authors contributed equally to this work.
[#]Present addresses: Department of Medical Biotechnology, Division of Biomedical Convergence, Kangwon National University, Chuncheon 24341, Republic of Korea

Supporting Information

The Supporting Information is available free of charge on the ACS Publications website at DOI: 10.1021/acs.nano-lett.XXXXXXX. Detailed information about materials and methods; stability in solution (Figure S1); characterization of the CCV and CCV/MPLA formulations (Figure S2); *in vitro* safety (Figure S3); *in vivo* transport (Figure S4); prophylactic efficacy in a colorectal cancer model (Figure S5); importance of antigen and adjuvant co-localization for prophylactic efficacy (Figure S6); therapeutic efficacy in a colorectal cancer model (Figure S7); therapeutic efficacy in an established colorectal cancer model (Figure S8); characterization of a B16F10 CCND formulation (Figure S9) (PDF)

The authors declare no competing financial interest.

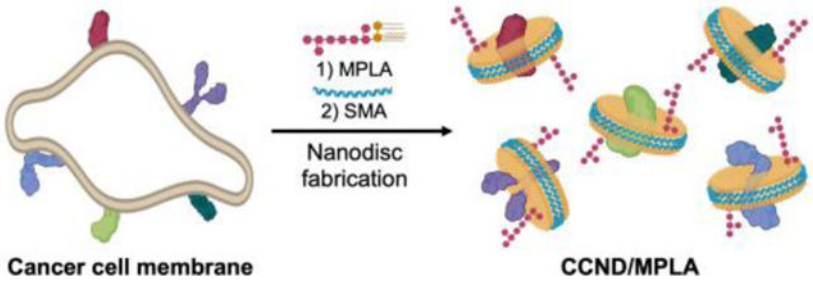

Keywords

anticancer vaccination; cancer immunotherapy; nanodisc; cellular nanoparticle; nanoparticle delivery; checkpoint blockade

Immunotherapy has altered the clinical landscape of cancer treatment, helping to revolutionize the management of certain types of malignancies and greatly improving patient survival.[1–2] Along these lines, modalities such as immune checkpoint blockade and adoptive cell transfer have demonstrated considerable promise, receiving numerous approvals from the United States Food and Drug Administration (FDA).[3–4] Therapeutic vaccines aimed at eliciting tumor antigen-specific immune responses are another form of cancer immunotherapy that have been widely explored, but unfortunately their clinical success thus far has been limited.[5–6] Although the FDA approval of sipuleucel-T, an antigen-pulsed autologous dendritic cell vaccine for the treatment of prostate cancer, represented a landmark achievement in the field, its clinical adoption was underwhelming.[7–8] A major challenge with designing an effective anticancer vaccine is the weakly immunogenic nature of most established tumors.[9] Additionally, their immunosuppressive microenvironments make tumors highly adept at evading destruction by effector immune cells.[10–11]

Given the challenges facing the development of therapeutic cancer vaccines, there has been considerable interest in novel nanotechnologies that can be used to further boost antitumor immune responses.[12] One approach for overcoming the low immunogenicity of cancer cells has been to leverage nanoparticulate carriers capable of co-delivering tumor antigens along with potent immunological adjuvants to antigen-presenting cells (APCs).[13–14] Cell membrane-based nanoparticles are an emerging platform capable of mimicking a wide range of cellular properties that can be leveraged for biomedical applications,[15–17] including vaccine design.[18–19] They have been successfully fabricated from red blood cells (RBCs), platelets, and white blood cells, among many others.[20–31] In particular, cancer cell membrane-coated nanoparticles represent a promising platform for anticancer vaccination that is inherently multiantigenic and can elicit robust antitumor immunity.[32–40] Another important consideration when developing nanovaccines is their size, which dictates how efficiently the particles transport to the lymph nodes and interact with resident immune cells.[41] Among the various classes of nanoparticles, nanodiscs are particularly attractive for their small sub-20 nm size.[42] It has been previously demonstrated that nanodiscs can be incorporated with both antigen and adjuvant payloads for anticancer vaccination.[43]

Here, we report on the development of an anticancer vaccine platform comprised of nanodiscs synthesized directly from cancer cell membranes (denoted 'CCND') (Figure 1a). To fabricate CCNDs, a styrene–maleic acid (SMA) copolymer was used as a membrane scaffold, resulting in nanoparticles possessing a discoidal shape and small size that facilitated their effective accumulation in the draining lymph nodes after *in vivo* administration. To augment the immune response against the tumor antigens on CCNDs, a potent Toll-like receptor 4 (TLR4) agonist, monophosphoryl lipid A (MPLA), was incorporated. The final formulation (denoted 'CCND/MPLA') was effective at eliciting immune responses against the source cancer cells, significantly inhibiting tumor growth in both prophylactic and therapeutic settings using a murine model of colorectal cancer. The nanovaccine was also effective at preventing metastasis in a weakly immunogenic melanoma model. Overall, the use of cell membrane-based nanodiscs represents an exciting new avenue for anticancer vaccine development that may pave the way for improved cancer therapeutics.

RESULTS AND DISCUSSION

Preparation and Characterization of CCNDs.

To fabricate the CCND/MPLA formulation, plasma membrane from the MC38 murine colorectal cancer line was derived following a previous established protocol.[33] MPLA was then added to the membrane, followed by homogenization using a probe sonicator. To form nanodiscs, the mixture was vortexed with SMA overnight, and any non-solubilized membrane and MPLA was removed via ultracentrifugation. Lastly, centrifugal ultrafiltration devices were used to eliminate excess SMA and concentrate the final CCND/MPLA product. After these preparation steps, it was determined that MPLA was incorporated at approximately 1.8 wt% with respect to the CCND protein content, and 46% of the inputted cancer antigens were retained in the final formulation. Whereas both CCNDs and the CCND/MLPA formulation exhibited a size of 16 nm when measured by dynamic light scattering (Figure 1b), CCND/MPLA had a more negative zeta potential of −20 mV (Figure 1c). In terms of stability, there were no significant changes in the size of CCND/MPLA when stored in phosphate-buffered saline (PBS) over the course 6 days (Figure S1). To visualize their structure, transmission electron microscopy was employed, revealing a relatively homogenous distribution of circular particles (Figure 1d), which was consistent with previous cell membrane-derived nanodisc works.[44] After subjecting the nanodisc samples to gel electrophoresis, it was observed that they possessed protein profiles similar to the MC38 plasma membrane (Figure 1e). Subsequently, western blotting analysis was used to confirm the presence of the tumor-promoting markers CD44 and programmed death ligand 1 (PD-L1),[45–46] as well as the tumor-associated antigen EphA2[47] (Figure 1f). As controls, MC38 cancer cell membrane vesicles (denoted 'CCV') and CCVs incorporated with MPLA (denoted 'CCV/MPLA') were also fabricated (Figure S2).

In Vitro Uptake and Immune Stimulation.

After confirming the successful fabrication of CCND/MPLA, we evaluated the immunogenicity of the formulation *in vitro* using bone marrow-derived dendritic cells (BMDCs). First, the uptake efficiency of the nanodiscs was compared with that of their

vesicular counterparts by labeling each with a far-red fluorophore. When analyzed by flow cytometry, it was observed that the CCNDs, either with or without MPLA, were much more effectively taken up by the BMDCs over time compared with the corresponding CCV formulations at the same protein and MPLA concentrations, particularly within the first 2 h (Figure 2a). The increased uptake of the nanodiscs was corroborated by fluorescence microscopy images of BMDCs after incubation with CCND/MPLA or CCV/MPLA for 3 h (Figure 2b). It was confirmed that CCND/MPLA did not have any cytotoxic effects when incubated with BMDCs over an extended period of 2 days (Figure S2). Next, the immunostimulatory properties of CCND/MPLA were assessed by incubating the formulation with BMDCs *in vitro* for 2 days. For these experiments, free MPLA, CCNDs, and RBC membrane nanodiscs[48] loaded with MPLA (denoted 'RBCND/MPLA') were employed at equivalent protein and/or MPLA concentrations as control groups. When analyzing the maturation markers CD40, CD80, CD86, and major histocompatibility complex (MHC)-II, the BMDCs incubated with CCND/MPLA exhibited the highest expression (Figure 2c–f). While all MPLA-containing samples exhibited some degree of immunostimulatory capacity, the superiority of CCND/MPLA suggests that the incorporation of MPLA into moderately immunogenic cancer cell membrane in a nanodisc format likely improves the interaction of the adjuvant with its cognate TLR. Using enzyme-linked immunosorbent assays (ELISAs), the *in vitro* production of the proinflammatory cytokines interleukin (IL)-6 and IL-12p40 by BMDCs was also assessed (Figure 2g,h). Consistent with the maturation marker expression, the highest cytokine levels were observed from cells incubated with the CCND/MPLA formulation for 2 days. Overall, these *in vitro* results provided a positive indication that CCND/MPLA could be used as a nanovaccine.

In Vivo Transport and Cellular Localization.

Following verification of the *in vitro* immunostimulatory capacity of CCND/MPLA, we next sought to evaluate its performance *in vivo*. First, the transport characteristics of the formulation was evaluated by administering dye-labeled CCV/MPLA or CCND/MPLA at the same protein and MPLA concentrations into mice via the hock and collecting the draining popliteal lymph node (PLN) at different timepoints. At 6 h after injection, it was observed by ex vivo imaging that more of the nanodisc formulation was present in the PLNs than the membrane vesicle formulation by a factor of approximately 2-fold (Figure S3a,b). When analyzing individual immune cell populations in the PLN using flow cytometry, antigen-presenting cells such as dendritic cells, macrophages, and B cells were responsible for the majority of the uptake, which was much higher in magnitude for the nanodisc formulation (Figure S3c). Further analysis of the PLN at 24 h after injection revealed that the difference between the two groups was even more pronounced, with approximately 7-fold higher uptake for the nanodiscs versus the membrane vesicles (Figure 3a,b). Significantly higher uptake was also observed for all immune cell populations that were analyzed (Figure 3c). These results clearly showed the advantage of the nanodisc formulation in terms of *in vivo* transport characteristics, with the smaller size of the particles promoting more efficient lymphatic drainage after administration.

In Vivo Immune Stimulation.

To confirm the ability of the nanodiscs to stimulate immune cells *in vivo*, mice were subcutaneously vaccinated with the CCND/MPLA formulation and various controls at the same protein and MPLA concentrations via the hock. After 2 days, the $CD11c^+$ dendritic cell population in the PLN were analyzed by flow cytometry for expression of the maturation markers CD40, CD80, CD86, and MHC-II (Figure 3d–g). In this case, both RBCND/MPLA and CCND/MPLA were effective at promoting dendritic cell maturation, likely due to their enhanced transport and accumulation within the PLN. Conversely, neither CCND without adjuvant nor free MPLA showed significant immunostimulatory activity at the dosages that were employed for the study. To evaluate the generation of tumor antigen-specific immune responses, mice were vaccinated subcutaneously in the hock with CCND/MPLA and various controls at the same protein and MPLA concentrations on days 0 and 7. Then, splenocytes from the vaccinated mice were collected on day 28 and restimulated with tumor lysate (Figure 3h,i) or the Adpgk neoantigen peptide (Figure 3j,k). In this case, only the CCND/MPLA formulation was able to significantly upregulate the proportion of $CD8^+$ T cells positive for interferon γ (IFNγ) expression after 24 h of restimulation. The results in each case were corroborated by ELISAs quantifying the level of IFNγ secretion by the restimulated splenocytes after 7 days. In contrast to the dendritic cell maturation results, vaccination with RBCND/MPLA did not elevate antigen-specific cellular immunity, confirming that the cancer cell membrane component was critical in producing the observed results. Overall, with their ability to effectively co-deliver tumor antigens along with a potent adjuvant for immune processing *in vivo*, CCND/MPLA were able to promote tumor-targeted adaptive immune responses.

Prophylactic and Therapeutic Efficacy in a Colorectal Cancer Model.

We next proceeded to evaluate the ability of CCND/MPLA to inhibit tumor growth in a prophylactic setting using a murine model of colorectal cancer (Figure 4a,b and Figure S4). First, C57BL/6 mice were subcutaneously vaccinated twice 1 week apart with CCND/MPLA and various controls at equivalent protein and MPLA doses, followed by intradermal implantation with MC38 cells after another week. It was observed that tumor growth in mice vaccinated with CCND/MPLA was significantly delayed, whereas vaccination with free MPLA, RBCND/MPLA, and CCND had no impact. The difference was also reflected in the survival data, where prior vaccination with CCND/MPLA extended the median survival time to 27 days compared to 17 days for the control groups. We also confirmed the necessity of formulating MPLA into the nanodiscs, as co-administration of CCND with free MPLA at the same protein and MPLA concentrations was not nearly as effective at inhibiting tumor growth as CCND/MPLA (Figure S6).

After confirming that CCND/MPLA vaccination could produce effective immunity against live tumors, we investigated the ability of the nanodisc formulation to control tumor growth in a more challenging therapeutic scenario (Figure 4c,d and Figure S5). Here, MC38 cancer cells were first intradermally implanted into C57BL/6 mice, followed by subcutaneous treatment close to the tumor site with CCND/MPLA and various controls at the same protein and MPLA dose on days 2, 4, 6, 8, and 10 after tumor inoculation. In addition, antibodies against PD-L1 (αPD-L1) were intraperitoneally administered for select groups on days 2,

6, and 10. It was observed that, when provided therapeutically, CCND/MPLA could only inhibit tumor growth when supplemented with checkpoint blockade therapy using αPD-L1. Neither αPD-L1 alone, CCND/MPLA alone, nor RBCND/MPLA with αPD-L1 produced any meaningful delay in the tumor growth kinetics, highlighting the important role of the immunosuppressive microenvironment in promoting tumor progression. Treatment using CCND/MPLA with αPD-L1 significantly extended the median survival time to 37 days versus 22 days for the untreated control group, with one mouse experiencing complete tumor regression over the period of the study. Therapeutic efficacy was further confirmed in an established MC38 model in which the tumors were allowed to reach ~100 mm^3 in size prior to the start of treatment (Figure S8). Considerable control of tumor growth was again achieved using CCND/MPLA with αPD-L1, and the combination therapy was able to prolong median survival time from 21 days for the untreated controls to 29 days.

To probe into the mechanism behind the results for the therapeutic efficacy study, we examined regulatory T cell and effector T cell populations within the tumors (Figure 4e,f) and draining lymph node (Figure 4g,h). For these experiments, MC38 cancer cells were intradermally implanted onto the right flank of mice, and treatments were applied via the same routes as above on day 6. On day 10 of the study, the tumors and draining inguinal lymph nodes were extracted and processed into single-cell suspensions for flow cytometry. Consistent with the therapeutic efficacy findings, it was observed that CCND/MPLA treatment combined with αPD-L1 checkpoint blockade therapy reduced the percentage of $FoxP3^+$ $CD4^+$ regulatory T cells while increasing the proportion of $IFN\gamma^+$ $CD8^+$ effector T cells in both tissue samples. Of the various controls, CCND/MPLA treatment without checkpoint blockade also reduced the regulatory T cells but did not have a major impact on effector T cells. Notably, αPD-L1 alone or in combination with RBCND/MPLA had little effect on either cell population, highlighting the importance of combining a proper antigen-specific vaccination strategy with checkpoint blockade therapy.

Therapeutic Efficacy in a Metastatic Melanoma Model.

To demonstrate the broad applicability of the CCND platform, we investigated its therapeutic efficacy in a metastatic melanoma model. Weakly immunogenic B16F10 murine melanoma cells expressing luciferase were administered via the tail vein, and then CCND/MPLA or various controls at the same protein and MPLA dose were subcutaneously administered on days 2, 4, 6, 8, and 10 after tumor inoculation. As before, αPD-L1 was administered intraperitoneally on days 2, 6, and 10 for the appropriate groups. Here, the CCNDs were prepared using B16F10 membrane, and it was confirmed that all formulations had similar physicochemical properties compared to those generated using MC38 membrane (Figure S6). Metastatic tumor growth was monitored over time via bioluminescence using a live animal imaging system (Figure 5a,b). Significant signal was detected on day 20 in mice for all control groups, including those administered with αPD-L1 only, CCND/MPLA only, or RBCND/MPLA with αPD-L1. In contrast, significantly lower luminescence was detected for mice receiving CCND/MPLA with αPD-L1. The results were even more striking when visualizing and quantifying the number of metastatic nodules in the lungs of each mouse on day 29 (Figure 5c,d). On average, mice vaccinated with CCND/MPLA and receiving supplemental αPD-L1 had 15 nodules, whereas mice receiving control treatments

and no treatment had approximately 60 and 80 nodules, respectively. Overall, these results confirmed that the CCND vaccine platform, when used in conjunction with checkpoint blockade therapy, could be generalized to other cancer types and provide therapeutic efficacy even against weakly immunogenic tumors.

CONCLUSION

We fabricated CCNDs incorporated with a strong immunological adjuvant as a platform for anticancer vaccination. The resulting formulation exhibited a small size that enabled efficient co-delivery of the multiantigenic membrane material and adjuvant to the draining lymph nodes for immune processing. It was confirmed that CCND/MPLA were effective at inducing the maturation of antigen-presenting cells, initiating a process that culminated in the generation of tumor antigen-specific cellular immune responses. As a result, the nanovaccine was effective at controlling tumor growth in a colorectal cancer model when used in a prophylactic setting. In more challenging therapeutic scenarios, CCND/MPLA alone had no impact on tumor growth, but significant efficacy was achieved against multiple tumor models when combining the nanovaccine with checkpoint blockade therapy. These findings highlight the promise of combinatorial immunotherapeutic approaches for cancer treatment, where different aspects of the antitumor immune response can be augmented simultaneously to achieve improved outcomes. In the future, it may be possible to generate CCND formulations directly from a patient's resected tumor material, thus enabling the platform to be used for personalized cancer immunotherapy. While much work still needs to be done, the use of cell membrane nanodiscs represents a promising approach for pushing forward the development of anticancer nanovaccines that may eventually find utility in the clinic.

Supplementary Material

Refer to Web version on PubMed Central for supplementary material.

ACKNOWLEDGEMENTS

This work was supported by the Defense Threat Reduction Agency Joint Science and Technology Office for Chemical and Biological Defense under award number HDTRA1-21-1-0010 and the National Institutes of Health under Award Number R21AI159492.

REFERENCES

(1). Egen JG; Ouyang W; Wu LC, Human anti-tumor immunity: Insights from immunotherapy clinical trials. Immunity 2020, 52, 36–54. [PubMed: 31940272]

(2). DeBerardinis RJ, Tumor microenvironment, metabolism, and immunotherapy. N. Engl. J. Med 2020, 382, 869–871. [PubMed: 32101671]

(3). Korman AJ; Garrett-Thomson SC; Lonberg N, The foundations of immune checkpoint blockade and the ipilimumab approval decennial. Nat. Rev. Drug Discov 2022, 21, 509–528. [PubMed: 34937915]

(4). Waldman AD; Fritz JM; Lenardo MJ, A guide to cancer immunotherapy: From T cell basic science to clinical practice. Nat. Rev. Immunol 2020, 20, 651–668. [PubMed: 32433532]

(5). Melero I; Gaudernack G; Gerritsen W; Huber C; Parmiani G; Scholl S; Thatcher N; Wagstaff J; Zielinski C; Faulkner I; Mellstedt H, Therapeutic vaccines for cancer: An overview of clinical trials. Nat. Rev. Clin. Oncol 2014, 11, 509–524. [PubMed: 25001465]

(6). Saxena M; van der Burg SH; Melief CJM; Bhardwaj N, Therapeutic cancer vaccines. Nat. Rev. Cancer 2021, 21, 360–378. [PubMed: 33907315]

(7). Sabado RL; Balan S; Bhardwaj N, Dendritic cell-based immunotherapy. Cell Res. 2017, 27, 74–95. [PubMed: 28025976]

(8). Caram MEV; Ross R; Lin P; Mukherjee B, Factors associated with use of sipuleucel-T to treat patients with advanced prostate cancer. JAMA Netw. Open 2019, 2, e192589. [PubMed: 31002323]

(9). Hu Z; Ott PA; Wu CJ, Towards personalized, tumour-specific, therapeutic vaccines for cancer. Nat. Rev. Immunol 2018, 18, 168–182. [PubMed: 29226910]

(10). Binnewies M; Roberts EW; Kersten K; Chan V; Fearon DF; Merad M; Coussens LM; Gabrilovich DI; Ostrand-Rosenberg S; Hedrick CC; Vonderheide RH; Pittet MJ; Jain RK; Zou W; Howcroft TK; Woodhouse EC; Weinberg RA; Krummel MF, Understanding the tumor immune microenvironment (TIME) for effective therapy. Nat. Med 2018, 24, 541–550. [PubMed: 29686425]

(11). Togashi Y; Shitara K; Nishikawa H, Regulatory T cells in cancer immunosuppression - Implications for anticancer therapy. Nat. Rev. Clin. Oncol 2019, 16, 356–371. [PubMed: 30705439]

(12). Zhao L; Seth A; Wibowo N; Zhao CX; Mitter N; Yu C; Middelberg AP, Nanoparticle vaccines. Vaccine 2014, 32, 327–37. [PubMed: 24295808]

(13). Fang RH; Kroll AV; Zhang L, Nanoparticle-based manipulation of antigen-presenting cells for cancer immunotherapy. Small 2015, 11, 5483–5496. [PubMed: 26331993]

(14). Sahdev P; Ochyl LJ; Moon JJ, Biomaterials for nanoparticle vaccine delivery systems. Pharm. Res 2014, 31, 2563–2582. [PubMed: 24848341]

(15). Fang RH; Jiang Y; Fang JC; Zhang L, Cell membrane-derived nanomaterials for biomedical applications. Biomaterials 2017, 128, 69–83. [PubMed: 28292726]

(16). Fang RH; Kroll AV; Gao W; Zhang L, Cell membrane coating nanotechnology. Adv. Mater 2018, 30, 1706759.

(17). Fang RH; Gao W; Zhang L, Targeting drugs to tumours using cell membrane-coated nanoparticles. Nat. Rev. Clin. Oncol 2023, 20, 33–48. [PubMed: 36307534]

(18). Kroll AV; Jiang Y; Zhou J; Holay M; Fang RH; Zhang L, Biomimetic nanoparticle vaccines for cancer therapy. Adv. Biosyst 2019, 3, 1800219.

(19). Zhou J; Kroll AV; Holay M; Fang RH; Zhang L, Biomimetic nanotechnology toward personalized vaccines. Adv. Mater 2020, 32, 1901255.

(20). Hu CM; Zhang L; Aryal S; Cheung C; Fang RH; Zhang L, Erythrocyte membrane-camouflaged polymeric nanoparticles as a biomimetic delivery platform. Proc. Natl. Acad. Sci. U. S. A 2011, 108, 10980–10985. [PubMed: 21690347]

(21). Hu CM; Fang RH; Copp J; Luk BT; Zhang L, A biomimetic nanosponge that absorbs pore-forming toxins. Nat. Nanotechnol 2013, 8, 336–340. [PubMed: 23584215]

(22). Parodi A; Quattrocchi N; van de Ven AL; Chiappini C; Evangelopoulos M; Martinez JO; Brown BS; Khaled SZ; Yazdi IK; Enzo MV; Isenhart L; Ferrari M; Tasciotti E, Synthetic nanoparticles functionalized with biomimetic leukocyte membranes possess cell-like functions. Nat. Nanotechnol 2013, 8, 61–68. [PubMed: 23241654]

(23). Hu CM; Fang RH; Wang KC; Luk BT; Thamphiwatana S; Dehaini D; Nguyen P; Angsantikul P; Wen CH; Kroll AV; Carpenter C; Ramesh M; Qu V; Patel SH; Zhu J; Shi W; Hofman FM; Chen TC; Gao W; Zhang K, et al. , Nanoparticle biointerfacing by platelet membrane cloaking. Nature 2015, 526, 118–121. [PubMed: 26374997]

(24). Hu Q; Sun W; Qian C; Wang C; Bomba HN; Gu Z, Anticancer platelet-mimicking nanovehicles. Adv. Mater 2015, 27, 7043–7050. [PubMed: 26416431]

(25). Gao C; Lin Z; Jurado-Sanchez B; Lin X; Wu Z; He Q, Stem cell membrane-coated nanogels for highly efficient in vivo tumor targeted drug delivery. Small 2016, 12, 4056–4062. [PubMed: 27337109]

(26). Thamphiwatana S; Angsantikul P; Escajadillo T; Zhang Q; Olson J; Luk BT; Zhang S; Fang RH; Gao W; Nizet V; Zhang L, Macrophage-like nanoparticles concurrently absorbing endotoxins and proinflammatory cytokines for sepsis management. Proc. Natl. Acad. Sci. U. S. A 2017, 114, 11488–11493. [PubMed: 29073076]

(27). Yu Z; Zhou P; Pan W; Li N; Tang B, A biomimetic nanoreactor for synergistic chemiexcited photodynamic therapy and starvation therapy against tumor metastasis. Nat. Commun 2018, 9, 5044. [PubMed: 30487569]

(28). Zhang Q; Dehaini D; Zhang Y; Zhou J; Chen X; Zhang L; Fang RH; Gao W; Zhang L, Neutrophil membrane-coated nanoparticles inhibit synovial inflammation and alleviate joint damage in inflammatory arthritis. Nat. Nanotechnol 2018, 13, 1182–1190. [PubMed: 30177807]

(29). Wang C; Wang Y; Zhang L; Miron RJ; Liang J; Shi M; Mo W; Zheng S; Zhao Y; Zhang Y, Pretreated macrophage-membrane-coated gold nanocages for precise drug delivery for treatment of bacterial infections. Adv. Mater 2018, 30, 1804023.

(30). Wu S; Huang Y; Yan J; Li Y; Wang J; Yang YY; Yuan P; Ding X, Bacterial outer membrane-coated mesoporous silica nanoparticles for targeted delivery of antibiotic rifampicin against Gram-negative bacterial infection in vivo. Adv. Funct. Mater 2021, 31, 2103442.

(31). Zhai Y; Wang J; Lang T; Kong Y; Rong R; Cai Y; Ran W; Xiong F; Zheng C; Wang Y; Yu Y; Zhu HH; Zhang P; Li Y, T lymphocyte membrane-decorated epigenetic nanoinducer of interferons for cancer immunotherapy. Nat. Nanotechnol 2021, 16, 1271–1280. [PubMed: 34580467]

(32). Fang RH; Hu CM; Luk BT; Gao W; Copp JA; Tai Y; O'Connor DE; Zhang L, Cancer cell membrane-coated nanoparticles for anticancer vaccination and drug delivery. Nano Lett. 2014, 14, 2181–2188. [PubMed: 24673373]

(33). Kroll AV; Fang RH; Jiang Y; Zhou J; Wei X; Yu CL; Gao J; Luk BT; Dehaini D; Gao W; Zhang L, Nanoparticulate delivery of cancer cell membrane elicits multiantigenic antitumor immunity. Adv. Mater 2017, 29, 1703969.

(34). Fontana F; Shahbazi MA; Liu D; Zhang H; Makila E; Salonen J; Hirvonen JT; Santos HA, Multistaged nanovaccines based on porous silicon@acetalated dextran@cancer cell membrane for cancer immunotherapy. Adv. Mater 2017, 29, 1603239.

(35). Yang R; Xu J; Xu L; Sun X; Chen Q; Zhao Y; Peng R; Liu Z, Cancer cell membrane-coated adjuvant nanoparticles with mannose modification for effective anticancer vaccination. ACS Nano 2018, 12, 5121–5129. [PubMed: 29771487]

(36). Liu WL; Zou MZ; Liu T; Zeng JY; Li X; Yu WY; Li CX; Ye JJ; Song W; Feng J; Zhang XZ, Cytomembrane nanovaccines show therapeutic effects by mimicking tumor cells and antigen presenting cells. Nat. Commun 2019, 10, 3199. [PubMed: 31324770]

(37). Jiang Y; Krishnan N; Zhou J; Chekuri S; Wei X; Kroll AV; Yu CL; Duan Y; Gao W; Fang RH; Zhang L, Engineered cell-membrane-coated nanoparticles directly present tumor antigens to promote anticancer immunity. Adv. Mater 2020, 32, 2001808.

(38). Chen L; Qin H; Zhao R; Zhao X; Lin L; Chen Y; Lin Y; Li Y; Qin Y; Li Y; Liu S; Cheng K; Chen H; Shi J; Anderson GJ; Wu Y; Zhao Y; Nie G, Bacterial cytoplasmic membranes synergistically enhance the antitumor activity of autologous cancer vaccines. Sci. Transl. Med 2021, 13, eabc2816. [PubMed: 34233949]

(39). Xu C; Jiang Y; Han Y; Pu K; Zhang R, A polymer multicellular nanoengager for synergistic NIR-II photothermal immunotherapy. Adv. Mater 2021, 33, 2008061.

(40). Johnson DT; Zhou J; Kroll AV; Fang RH; Yan M; Xiao C; Chen X; Kline J; Zhang L; Zhang DE, Acute myeloid leukemia cell membrane-coated nanoparticles for cancer vaccination immunotherapy. Leukemia 2022, 36, 994–1005. [PubMed: 34845316]

(41). Reddy ST; van der Vlies AJ; Simeoni E; Angeli V; Randolph GJ; O'Neil CP; Lee LK; Swartz MA; Hubbell JA, Exploiting lymphatic transport and complement activation in nanoparticle vaccines. Nat. Biotechnol 2007, 25, 1159–1164. [PubMed: 17873867]

(42). Denisov IG; Sligar SG, Nanodiscs for structural and functional studies of membrane proteins. Nat. Struct. Mol. Biol 2016, 23, 481–486. [PubMed: 27273631]

(43). Kuai R; Ochyl LJ; Bahjat KS; Schwendeman A; Moon JJ, Designer vaccine nanodiscs for personalized cancer immunotherapy. Nat. Mater 2017, 16, 489–496. [PubMed: 28024156]

(44). Noh I; Guo ZY; Zhou JR; Gao WW; Fang RH; Zhang LF, Cellular nanodiscs made from bacterial outer membrane as a platform for antibacterial vaccination. ACS Nano 2022, 17, 1120–1127.

(45). Noh I; Kim HO; Choi J; Choi Y; Lee DK; Huh YM; Haam S, Co-delivery of paclitaxel and gemcitabine via CD44-targeting nanocarriers as a prodrug with synergistic antitumor activity against human biliary cancer. Biomaterials 2015, 53, 763–774. [PubMed: 25890771]

(46). Juneja VR; McGuire KA; Manguso RT; LaFleur MW; Collins N; Haining WN; Freeman GJ; Sharpe AH, PD-L1 on tumor cells is sufficient for immune evasion in immunogenic tumors and inhibits CD8 T cell cytotoxicity. J. Exp. Med 2017, 214, 895–904. [PubMed: 28302645]

(47). Yamaguchi S; Tatsumi T; Takehara T; Sakamori R; Uemura A; Mizushima T; Ohkawa K; Storkus WJ; Hayashi N, Immunotherapy of murine colon cancer using receptor tyrosine kinase EphA2-derived peptide-pulsed dendritic cell vaccines. Cancer 2007, 110, 1469–1477. [PubMed: 17685394]

(48). Sun L; Wang D; Noh I; Fang RH; Gao W; Zhang L, Synthesis of erythrocyte nanodiscs for bacterial toxin neutralization. Angew. Chem. Int. Ed. Engl 2023, 62, e202301566. [PubMed: 36853913]

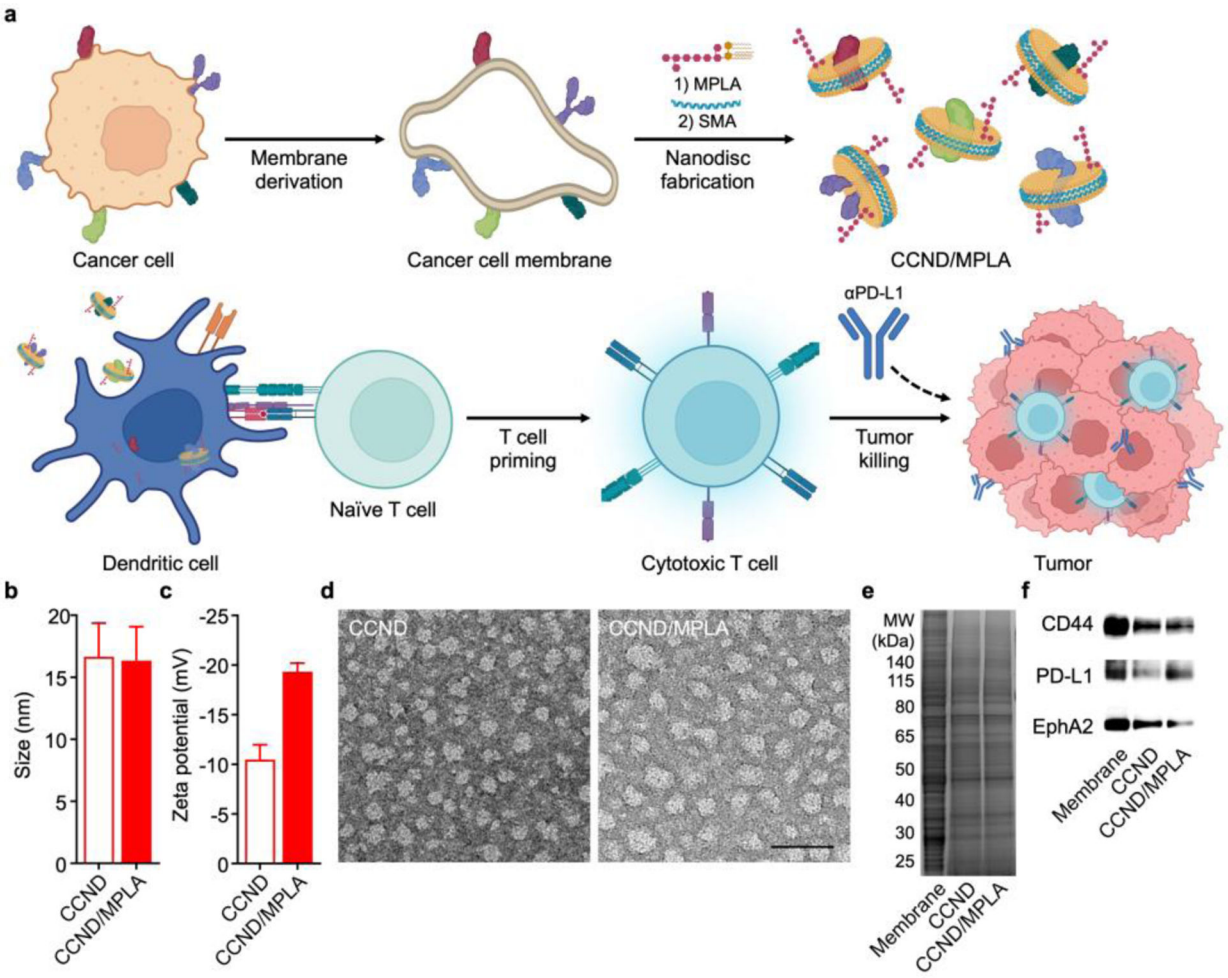

Figure 1.

Preparation and characterization of cancer cell membrane nanodisc (CCND) formulation. (a) Cancer cell membrane is derived from whole cancer cells, followed by incubation with MPLA and SMA to form MPLA-loaded CCND (CCND/MPLA). The resulting formulation readily interacts with dendritic cells, thus promoting tumor antigen presentation to prime antigen-specific T cells, which work in conjunction with checkpoint blockade therapy to control tumor growth. (b,c) Size (b) and zeta potential (c) of CCND and CCND/MPLA (n = 3, mean + SD). (d) Transmission electron microscopy images of CCND (left) and CCND/MPLA (right) negatively stained with uranyl acetate (scale bar: 50 nm). (e) Protein profiles of MC38 cell membrane, CCND, and CCND/MPLA after gel electrophoresis. (f) Western blot probing for tumor antigens in MC38 cell membrane, CCND, and CCND/MPLA.

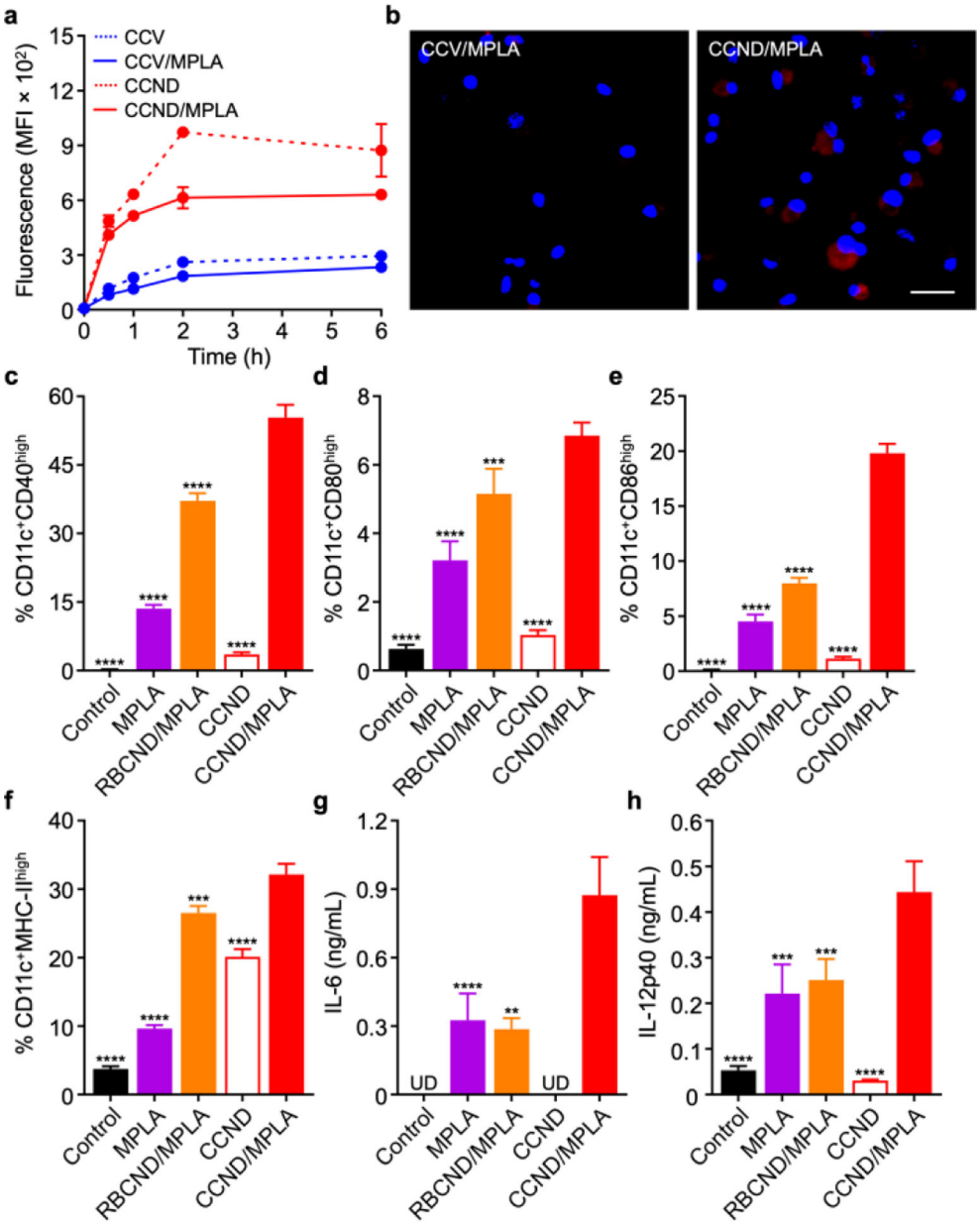

Figure 2.

In vitro uptake and immune stimulation. (a) Uptake of dye-labeled cancer cell vesicles (CCV), MPLA-loaded cancer vesicles (CCV/MPLA), CCND, and CCND/MPLA by BMDCs over time (n = 3, mean ± SD). (b) Fluorescence visualization of dye-labeled CCV/MPLA (left) and CCND/MPLA (right) uptake after 3 h of incubation with BMDCs (scale bar: 20 μm; red: CCV/MPLA or CCND/MPLA, blue: nuclei). (c-f) Expression of the maturation markers CD40 (c), CD80 (d), CD86 (e), and MHC-II (f) by BMDCs after 2 days of incubation with MPLA, MPLA-loaded RBC nanodiscs (RBCND/MPLA), CCND, and CCND/MPLA (n = 3, mean + SD). (g,h) Concentration of IL-6 (g) and IL-12p40 (h) secreted by BMDCs after 2 days of incubation with CCND/MPLA and various controls

(UD: undetectable; n = 3, mean + SD). $^{**}p < 0.01$, $^{***}p < 0.001$, $^{****}p < 0.0001$ (compared to CCND/MPLA); one-way ANOVA.

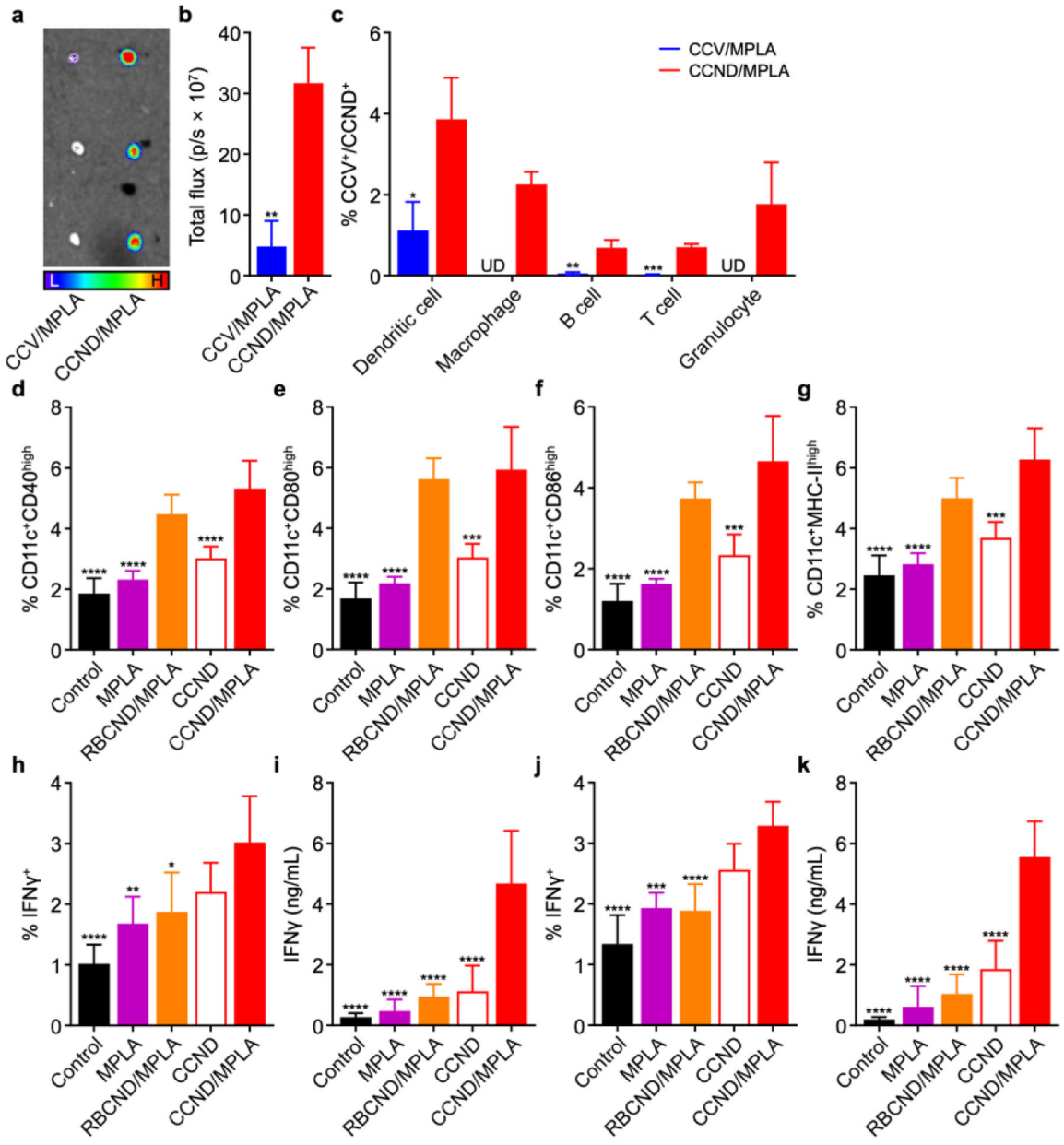

Figure 3.

In vivo transport and immune stimulation. (a) Ex vivo fluorescent imaging of the draining PLN at 24 h after the administration of dye-labeled CCV/MPLA and CCND/MPLA (L: low signal, H: high signal). (b) Quantification of fluorescence in the PLN at 24 h after the administration of dye-labeled CCV/MPLA and CCND/MPLA (n = 3, mean + SD). (c) Percentage of dendritic cells, macrophages, B cells, T cells, or granulocytes in the PLN positive for uptake of dye-labeled CCV/MPLA or CCND/MPLA at 24 h after administration (UD: undetectable; n = 3, mean + SD). (d–g) Expression of the maturation markers CD40 (d), CD80 (e), CD86 (f), and MHC-II (g) on dendritic cells in the draining PLN at 2 days after vaccination with CCND/MPLA and various controls (n = 5, mean + SD). (h–k) Percentage of IFNγ^+ cells in the CD8$^+$ T cell population (h,j) and IFNγ secretion level (i,k)

for splenocytes collected from mice on day 28 after immunization with CCND/MPLA and various controls on days 0 and 7, followed by restimulation with (h,i) MC38 lysate or (j,k) the Adpgk peptide (n = 5, mean + SD). *$p < 0.05$, **$p < 0.01$, ***$p < 0.001$, and ****$p < 0.0001$ (compared to CCND/MPLA); Student's *t*-test for (b,c) and one-way ANOVA for (d–k).

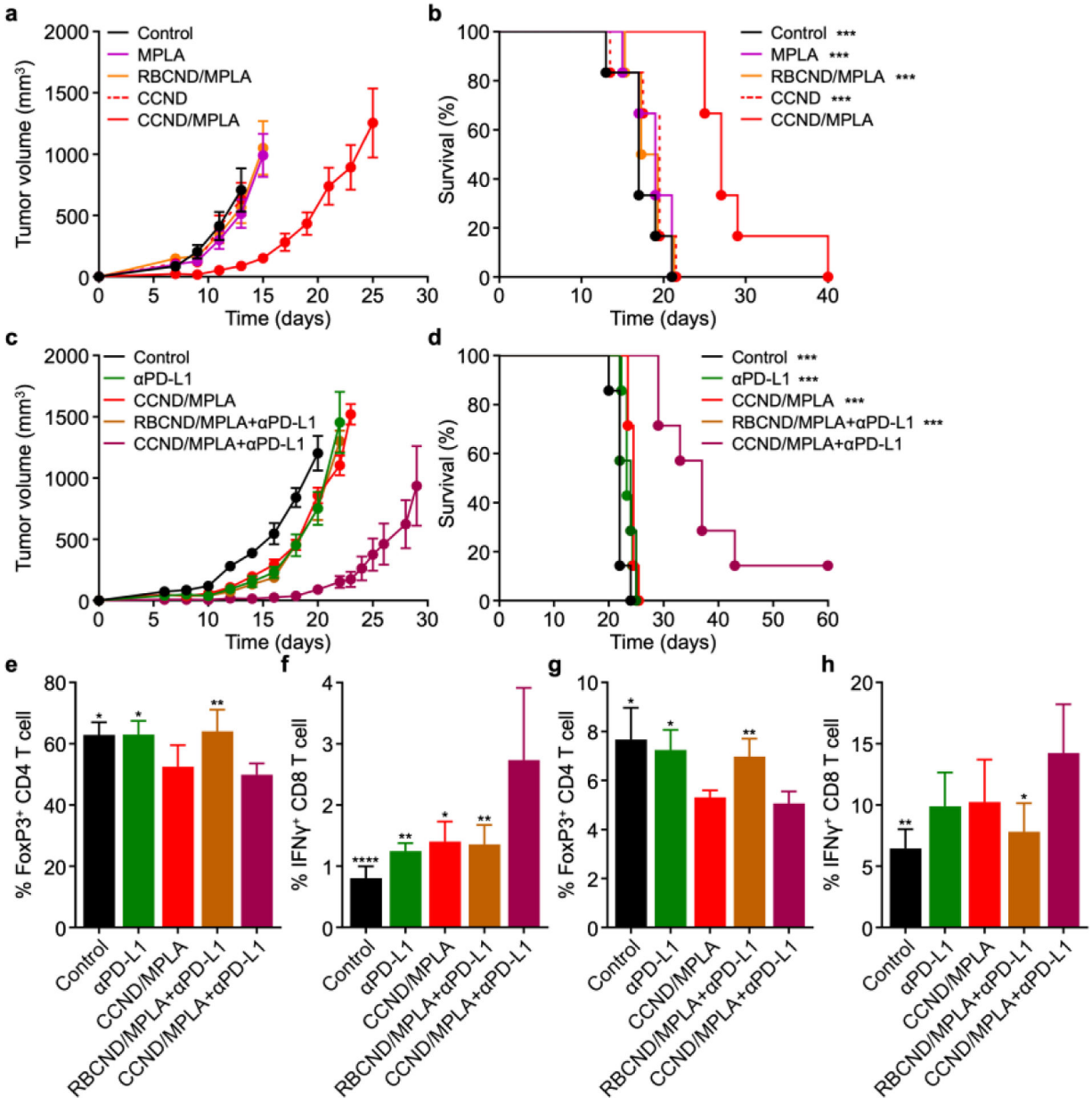

Figure 4.

Prophylactic and therapeutic efficacy in a colorectal cancer model. (a,b) Tumor growth kinetics (a) and overall survival (b) of mice subcutaneously immunized with CCND/MPLA and various controls on day −14 and day −7, followed by intradermal challenge with MC38 cells on the right flank on day 0 (n = 6, mean ± SEM). ***$p < .001$ (compared with CCND/MPLA); log-rank test. (c,d) Tumor growth kinetics (c) and overall survival (d) of mice intradermally challenged with MC38 cells on the right flank on day 0 and subcutaneously treated with CCND/MPLA and various controls on days 2, 4, 6, 8, and 10, along with αPD-L1 on days 2, 6, and 10 (n = 6, mean ± SEM). ***$p < .001$ (compared with CCND/MPLA+αPD-L1); log-rank test. (e–h) Percentage of $FoxP3^+$ $CD4^+$ T cells (e,g) and $IFN\gamma^+$ $CD8^+$ T cells (f,h) among the $CD3^+$ cell population in the tumors (e,f) and draining

inguinal lymph nodes (g,h) 10 days after intradermal challenge with MC38 cells; a single subcutaneous treatment using CCND/MPLA+αPD-L1 and various controls was performed on day 6 after tumor challenge (n = 4, mean + SD). *$p < 0.05$, **$p < 0.01$, and ****$p < 0.0001$ (compared to CCND/MPLA+αPD-L1); one-way ANOVA.

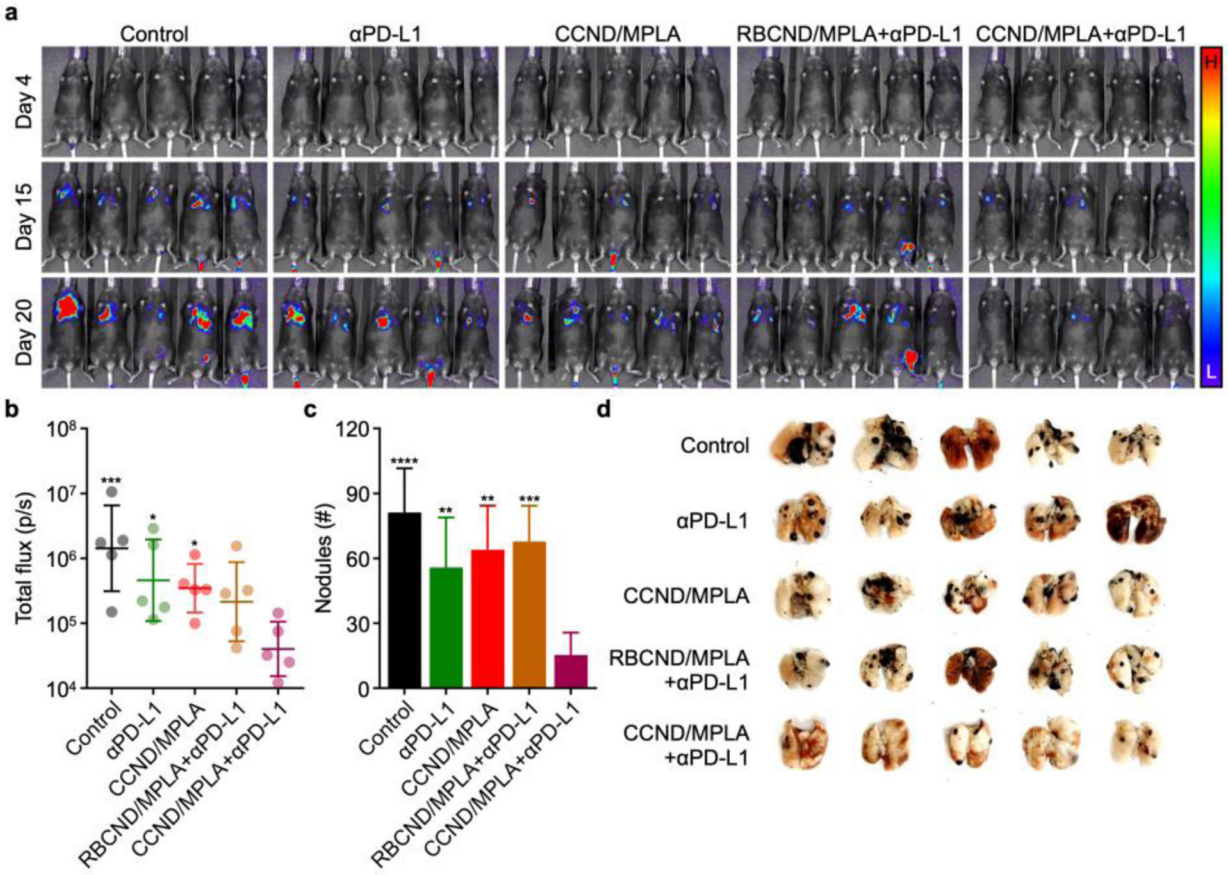

Figure 5.

Therapeutic efficacy in a metastatic melanoma model. (a) Bioluminescence imaging of mice intravenously challenged with luciferase-expressing B16F10 cells on day 0 and subcutaneously treated with CCND/MPLA (fabricated using B16F10 membrane) and various controls on days 2, 4, 6, 8, and 10, along with αPD-L1 on days 2, 6, and 10 (L: low signal, H: high signal). (b–d) Bioluminescence quantification on day 20 (b, geometric mean ± SD), metastatic nodule quantification on day 29 (c, mean + SD), and whole lung images on day 29 (d) for the mice in (a) (n = 5). *$p < 0.05$, **$p < 0.01$, ***$p < 0.001$, and ****$p < 0.0001$ (compared to CCND/MPLA+αPD-L1); one-way ANOVA.